

- <sup>1</sup>For example, S. D. Hersee, B. de Cremoux, and J. P. Duchemin, *Appl. Phys. Lett.* **44**, 476 (1984); T. Fujii, S. Yamakoshi, K. Nanbu, O. Wada, and S. Hiyamizu, *J. Vac. Sci. Technol. B* **2**, 259 (1984).
- <sup>2</sup>K. Woodbridge, P. Blood, E. D. Fletcher, and P. J. Hulyer, *Appl. Phys. Lett.* **45**, 16 (1984).
- <sup>3</sup>P. Blood, E. D. Fletcher, K. Woodbridge, and P. J. Hulyer, *Physica B* **129**, 465 (1985).
- <sup>4</sup>N. K. Dutta, *J. Appl. Phys.* **53**, 7211 (1982).
- <sup>5</sup>D. Kasemset, C-S. Hong, N. B. Patel, and P. D. Dapkus, *IEEE J. Quantum Electron.* **QE-19**, 1025 (1983).
- <sup>6</sup>K. Woodbridge, P. Dawson, J. P. Gowers, and C. T. Foxon, *J. Vac. Sci. Technol. B* **2**, 163 (1984).
- <sup>7</sup>G. Bastard, *Phys. Rev. B* **25**, 7584 (1982), as implemented in our laborato-

ry by G. Duggan (unpublished).

<sup>8</sup>R. L. Greene and K. K. Bajaj, *Solid State Commun.* **45**, 831 (1983).

<sup>9</sup>W. Streifer, D. R. Scifres, and R. D. Burnham, *Appl. Opt.* **18**, 3547 (1979).

<sup>10</sup>H. C. Casey Jr. and M. B. Panish, *Heterostructure Lasers* (Academic, New York, 1978), Part A, p. 183.

<sup>11</sup>In presentations of this data at the 1984 MBE conference (San Francisco) and the 1984 GaAs Symposium (Biarritz) the point for  $N = 2$  was incorrectly drawn. These data were obtained on a set of devices without a Zn diffused  $p$  contact and although the values of  $J_{th}$  differ slightly from those reported here (due to current spreading effects) these results also show  $J_{th}/d \approx \Gamma^{-1}$ .

<sup>12</sup>A. Sigmura, *IEEE J. Quantum Electron.* **QE-20**, 336 (1984).

## Lateral coupled cavity semiconductor laser

J. Salzman, R. Lang, and A. Yariv

*California Institute of Technology, Pasadena, California 91125*

(Received 28 March 1985; accepted for publication 21 May 1985)

We report the fabrication and operation of a *lateral* coupled cavity semiconductor laser that consists of two phase-locked parallel lasers of different lengths and with *separate* electrical contacts. Mode selectivity that results from the interaction between the two supermodes is investigated experimentally. Frequency selectivity and tunability are obtained by controlling the current to each laser separately. Highly stable single mode operation is also demonstrated.

Coupled cavity lasers have been used for frequency selection in a variety of multiresonator designs, including lasers coupled to external (passive) cavities,<sup>1,2</sup> lasers with internal partial reflections,<sup>3</sup> longitudinally coupled lasers,<sup>4,5</sup> and lasers coupled laterally to a passive cavity.<sup>6</sup> The possibility of mode control and frequency selectivity of laterally coupled cavities was demonstrated by Suematsu *et al.*<sup>6</sup>; however, in their vertically layered device, the optical properties of both cavities were controlled by the current from a single contact. It has been shown (in the C<sup>3</sup> laser,<sup>4</sup> for example) that mode control and frequency selectivity benefit from separate electrical control of the different cavities in the coupled system. Using the techniques we developed for etched mirrors, we have fabricated a laterally coupled cavity (LC<sup>2</sup>) laser consisting of two side-by-side lasers of different lengths with separate electrical contacts. The lasers are close enough together that their fields couple to one another. A description of their properties and an analysis follows.

Double heterostructure GaAs/GaAlAs wafers were grown by liquid phase epitaxy and laser stripes 4  $\mu\text{m}$  wide and with 9- $\mu\text{m}$  center separation were delineated by proton implantation [Fig. 1(a)]. The etching of the mirror in one of the stripes was accomplished by wet chemical etching using techniques previously described.<sup>10</sup>

Separate electrical contacts were provided by two Cr/Au pads evaporated on the  $p$  side. The fabrication process was completed by AuGe/Au evaporation on the  $n$  side and cleaving. The length of the two channel section,  $L$ , and of the additional single channel section,  $D$ , were determined by

cleaving, in the range of 200–400  $\mu\text{m}$  and 20–80  $\mu\text{m}$ , respectively.

Using a standard round trip analysis,<sup>7</sup> the self-reproducing modes of the resonator are linear combinations of the supermodes of the coupled waveguide system. The lasing frequencies are given by solutions to the following equation:

$$[r_{1\text{eff}} \exp(-2i\sigma_1 L) - 1][r_{2\text{eff}} \exp(-2i\sigma_2 L) - 1] = K_s,$$

where

$$r_{1\text{eff}} = \frac{r_1}{2}(1 + \alpha) + \frac{r_2}{2}(1 - \alpha)\exp(-2i\beta_3 D),$$

$$r_{2\text{eff}} = \frac{r_1}{2}(1 - \alpha) + \frac{r_2}{2}(1 + \alpha)\exp(-2i\beta_3 D),$$

$$K_s = \frac{1}{4}[r_2 \exp(-2i\beta_3 D) - r_1]^2 \times (1 - \alpha^2)\exp[-i(\beta_1 + \beta_2)L],$$

$$\alpha = \frac{\beta_2 - \beta_1}{\sigma_2 - \sigma_1},$$

$\beta_{1,2}, \sigma_{1,2}$  are the waveguide propagation constants and the supermode propagation constants, respectively,  $\beta_3$  is the propagation constant in the single channel section,  $r_{1,2}$  are the mirror reflectivities. [A schematic of the coordinate system, and the values  $r_i$  and  $\beta_i$  assumed in Eq. (1) is shown in Fig. 1(b).]

An analysis of the resonant frequencies as a function of the supermode gain predicted by Eq. (1) has been performed,<sup>8</sup> and frequency selectivity and tunability were predicted. The frequency selectivity can be understood by the

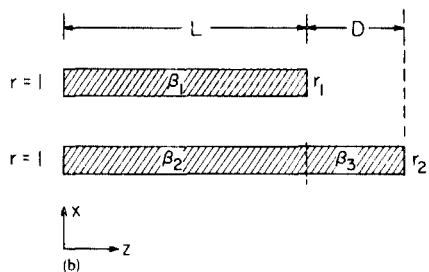
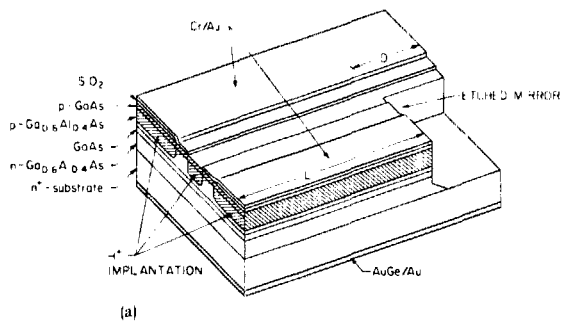
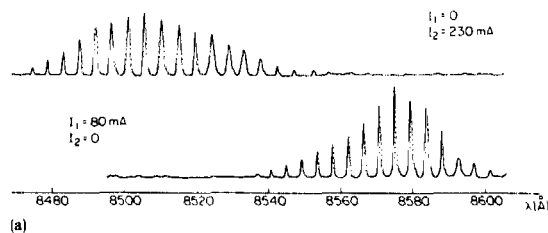


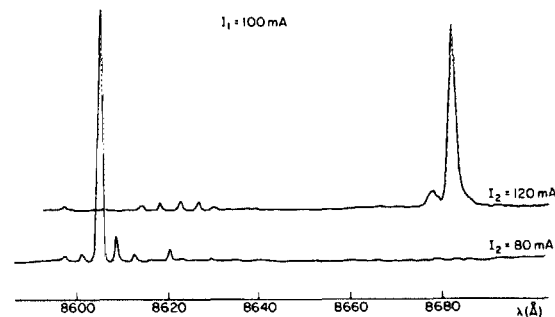
FIG. 1. Schematic picture of the LC<sup>2</sup> lasers.

following considerations. Let us assume first  $K_s \rightarrow 0$ . Then, setting each bracket of Eq. (1) equal to zero leads to the usual threshold condition for each supermode. [Namely, the gain  $g_i = \text{Im}(\sigma_i)$  should be equal to the loss  $(1/L)\ln(r_{i,\text{eff}})$ , and the phase  $\text{Re}(\sigma_i L)$  should be  $2N\pi$ , with  $N$  an integer.] But it is clear from the definition of  $r_{i,\text{eff}}$  that they are modulated by the factor  $\exp(-\beta_3 D)$ . This introduces the condition for maximum reflectivity  $\text{Re}(\beta_3 D) = 2M\pi$ . Thus, the loss of each supermode is modulated with a period which is different from that of the Fabry-Perot resonances, resulting in enhancement of lasing action only at the common frequencies. We consider next the finite value of  $K_s$ . Its effect is to couple the two supermodes in such a way that the lowest threshold is obtained when  $K_s$  is a positive number (the supermodes reinforce each other). Since the phase of  $K_s$  is changed by  $\exp(-2i\beta_3 D)$  and  $\exp[-i(\beta_1 + \beta_2)L]$ , the coupling is also frequency dependent. Thus, the effect of an additional length  $D$  in one of the waveguides is to provide (a) frequency-dependent effective reflectivity for each supermode and (b) a frequency-dependent coupling between the supermodes. These are the main physical mechanisms that result in mode suppression. In what follows, we describe an experimental demonstration of these properties.

In Fig. 2(a), the longitudinal spectra of the two component lasers when operated separately are plotted. The device lengths are  $L = 350 \mu\text{m}$  and  $D = 30 \mu\text{m}$ . A slight difference in the mode spacing (corresponding to the difference in length) can be noticed. When the shorter laser is operated above threshold, an injection current of  $I \sim 0.5I_{\text{th}}$  in the longer waveguide is sufficient to shift the spectrum toward longer wavelengths and to introduce a strong mode suppression. This is shown in Fig. 2(b). Furthermore, a slight increase in the current of the longer waveguide causes a mode hop of  $\Delta\lambda \sim 2\pi\lambda / \beta_3 D$ .<sup>9</sup> The effect of gain/loss modulation is better visualized in devices with larger values of  $D$ . This is shown in Fig. 3, in which the calculated modulating



(a)

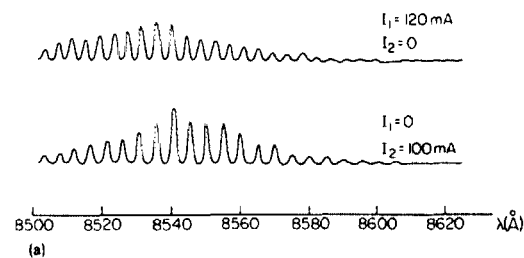


(b)

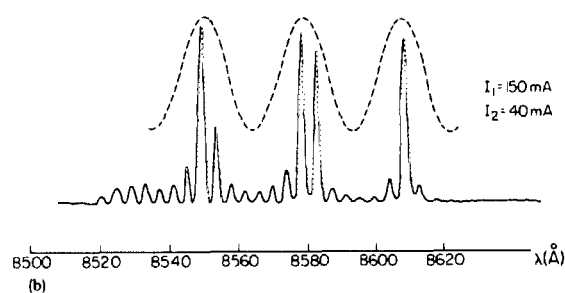
FIG. 2. (a) Longitudinal mode spectrum of each laser, when operated separately. (b) Spectrum of the LC<sup>2</sup> laser, when  $I_1 > I_{\text{th}}$  and  $I_2 \sim 0.5I_{\text{th}}$  for two different values of  $I_2$ . Note the shift toward longer wavelengths in comparison to the spectra in (a).

term (dotted line) has been superimposed over the observed spectrum. The effect of varying the current in one of the channels is shown in Fig. 4. Here, the relative phase between the two supermodes is changed, resulting in tuning of the combined resonances, and mode hopping.

Finally, we present in Fig. 5 an example of nearly single mode operation while the output power changed by a factor of  $\sim 2.5$ . We should mention that in this experiment the individual lasers were deliberately designed as gain-guided structures, possessing a multimode spectrum. Yet, the spec-



(a)



(b)

FIG. 3. (a) Longitudinal mode spectrum for each laser, when operated separately ( $L = 450 \mu\text{m}$ ,  $D = 60 \mu\text{m}$ ). (b) Spectrum of the LC<sup>2</sup> laser with the loss modulation function (dotted line).

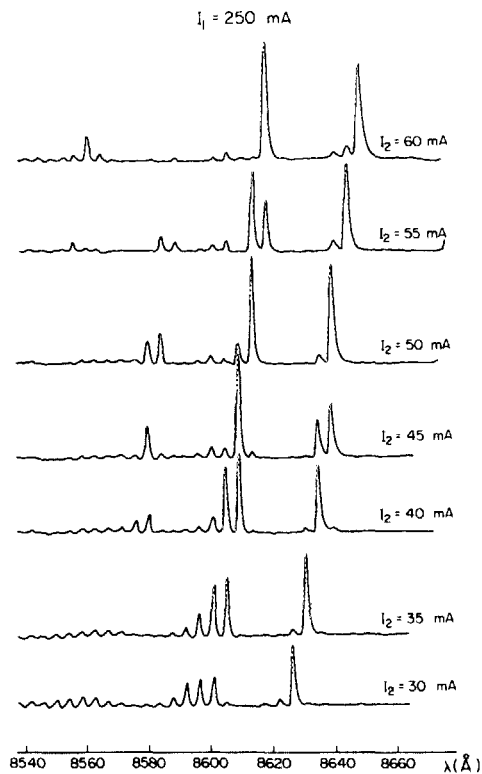


FIG. 4. Spectrum of the LC<sup>2</sup> laser (as in Fig. 3), showing tuning of the spectrum by varying the current  $I_2$ .

tra shown in Fig. 5 demonstrate that operating points can be found at which the LC<sup>2</sup> laser emission is in a single mode, with very high stability against changes in injection current (modulation) or temperature.

In conclusion, we have demonstrated that the LC<sup>2</sup> lasers have an inherent frequency selection capability that results from the modulation of the losses in different longitudinal modes. The loss modulation is a result of the complex reflectivity and of the coupling of the cavity supermodes which results from a nonuniform, frequency-dependent reflectivity. Frequency tuning or highly stable single mode operation can also be achieved by properly choosing the operating point.

In this experiment only one mirror was etched and the

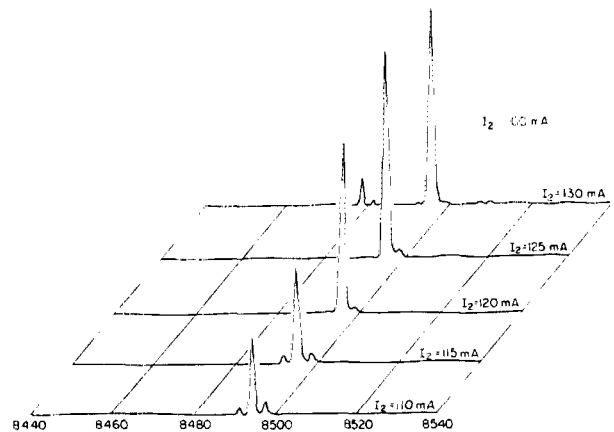


FIG. 5. Single mode operation of the LC<sup>2</sup> laser with continuous tuning by changing the current in one of the stripes.

other three mirrors were formed by cleaving, but the recent development of new etching techniques that result in smooth and vertical laser mirrors<sup>10</sup> can lead to a fully etched device, compatible with optoelectronic integration.

This research is supported by grants from the Army Research Office, the Air Force Office of Scientific Research, and the Office of Naval Research. J. Salzman would like to acknowledge the support of the Bantrell post-doctoral Fellowship and the Fullbright Fellowship. R. Lang would like to acknowledge the support of the National Science Foundation.

<sup>1</sup>R. P. Salathe, *Appl. Phys.* **20**, 1 (1979).

<sup>2</sup>C. Lin and C. A. Burrus, presented at the Topical Meeting on Optical Fiber Communication, New Orleans, Louisiana, Feb. 28–Mar. 2, 1983.

<sup>3</sup>H. K. Choi and S. Wang, *Appl. Phys. Lett.* **40**, 571 (1982).

<sup>4</sup>W. T. Tsang, N. A. Olsson, and R. A. Logan, *Appl. Phys. Lett.* **42**, 650 (1983).

<sup>5</sup>L. A. Coldren, B. I. Miller, K. Iga, and J. A. Rentschler, *Appl. Phys. Lett.* **38**, 315 (1981).

<sup>6</sup>Y. Suematsu, M. Yamada, and K. Hayashi, *IEEE J. Quantum Electron.* **QE-11**, 457 (1975).

<sup>7</sup>J. Salzman, R. Lang, and A. Yariv, *Opt. Lett.* **Aug.** (1985).

<sup>8</sup>R. Lang, J. Salzman, and A. Yariv (unpublished).

<sup>9</sup> $\Delta\lambda \sim 70 \text{ \AA}$ , which corresponds to the separation between the effective mirror maxima.

<sup>10</sup>J. Salzman, T. Venkatesan, S. Margalit, and A. Yariv, *J. Appl. Phys.* **57**, 2948 (1985).